Taylor, Christopher H. and Reader, Tom and Gilbert, Francis (2016) Why many Batesian mimics are inaccurate: evidence from hoverfly colour patterns. Proceedings of the Royal Society B: Biological Sciences, 283 (1842). pp. 1-8. ISSN 1471-2954

Title: Why many Batesian mimics are inaccurate: evidence from hoverfly colour patterns

Authors: Christopher H Taylor[1]

Tom Reader[1]

Francis Gilbert[1]

[1] School of Life Sciences, University of Nottingham, University Park, Nottingham, NG7 2RD

Corresponding author: Christopher Taylor

christopher.taylor@nottingham.ac.uk

ABSTRACT

Mimicry is considered a classic example of the elaborate adaptations that natural selection can produce, yet often similarity between Batesian (harmless) mimics and their unpalatable models is far from perfect. Variation in mimetic accuracy is a puzzle, since natural selection should favour mimics that are hardest to distinguish from their models. Numerous hypotheses exist to explain the persistence of inaccurate mimics, but most have rarely or never been tested against empirical observations from wild populations. One reason for this is the difficulty in measuring pattern similarity, a key aspect of mimicry.

Here, we use a recently developed method, based on the distance transform of binary images, to quantify pattern similarity both within and among species for a group of hoverflies and their hymenopteran models. This allowed us to test three key hypotheses regarding inaccurate mimicry. Firstly, we tested the prediction that selection should be more relaxed in less accurate mimics, but found that levels of phenotypic variation are similar across most hoverfly species. Secondly, we found no evidence that mimics have to compromise between accuracy to multiple model species. However we did find that darker-coloured hoverflies are less accurate mimics, which could lead to a trade-off between mimicry and thermoregulation in temperate regions. Our results shed light on a classic problem concerning the limitations of natural selection.

Keywords: Batesian mimicry; imperfect mimicry; Syrphidae; distance transform; thermal melanism.

INTRODUCTION

Charles Darwin regarded mimicry as a beautiful example of the extreme results of natural selection [1, p.392], and the topic has since been well studied as a powerful and conspicuous demonstration of the evolution of phenotypes [2]. Batesian mimics are harmless organisms that resemble a more dangerous "model" in order to deceive potential predators [3], and while some show an astonishing level of similarity to their models, others bear only a passing resemblance. Both theory [4] and experiments [5-7] show that, in practical terms, mimicry is a continuum rather than a simple binary category: inaccurate mimics are attacked less frequently than non-mimics, but more often than more accurate ones [but see 8, 9]. We would therefore expect the most accurate mimics in a population to have the highest fitness, and that natural selection should drive ever-increasing perfection in resemblance to the model. Contrary to this prediction, there are many examples, including some snakes [10], spiders [11] and hoverflies [12], that seem far from accurate in their mimicry. By exploring this discrepancy between expectation and observation, the study of inaccurate Batesian mimicry provides an excellent opportunity to develop a better understanding of the ecological forces which determine the evolution of phenotypes.

There is no shortage of hypotheses proposed to address the existence of inaccurate mimicry, and these have been well reviewed elsewhere [2, 13-15]. Here, we test some of the key hypotheses using hoverflies (Diptera: Syrphidae) as our study organisms, but the hypotheses are equally relevant to other groups of mimics. Hoverflies have been a major focus for studies of inaccurate mimicry, as the taxon comprises a large number of species, many of which are abundant and widespread, ranging from non-mimetic to highly accurate mimics of various hymenopteran models, with a wide range of inaccurate mimics in between [12, 15]. Hoverflies overlap their models extensively in space (with models such as *Apis mellifera* and *Vespula vulgaris* being widespread in the Palearctic), and also in time. Most species of hoverfly first emerge between March and May and remain active until at least September [16], with workers of social Hymenoptera generally reaching peak abundance in July/August [17].

Theoretical explanations for inaccurate Batesian mimicry have produced a number of testable predictions about variation within and among mimetic species. An important group of predictions centre on the

cognition and behaviour of the predator, which can be modelled using Signal Detection Theory [4]. This assumes that predators receive information from signals subject to noise, and therefore uncertainty. Signal Detection Theory suggests that, past a certain minimum level of similarity, further improvements in mimetic accuracy provide very little decrease in predation risk [18]. Mimics that have reached this critical level of similarity will therefore experience relaxed selection. From this, Holloway et al. [19] make the prediction that more accurate mimics should show greater phenotypic variation. They suggest that less accurate mimics are under strong selection but lack the genetic variation to evolve closer similarity to the model, and hence have low phenotypic variation.

However, alternative predictions arise if we consider that mimic species may not all be equally attractive to predators. The threshold similarity level described above, beyond which selection is relaxed [18], depends on what has been described as the "incentive to attack" [20]. A predator is less likely to risk an attack with an uncertain outcome if the cost of attacking a model is high relative to the benefit of consuming a mimic, or if the abundance of models is high relative to the mimics. One possible cause of low incentive to attack is given by Penney et al. [21], who argue that smaller mimics have a lower calorific value to the predator, resulting in a low incentive to attack, and hence favouring relatively imperfect mimicry in smaller species. Regardless of the exact reasons behind the costs and benefits to a predator, if a certain group of mimics offer a low incentive to attack, they are predicted to be under relatively relaxed selection by predators compared with other species, and may therefore show greater phenotypic variability.

We must also consider that predators may be influenced by more than one model phenotype. Mathematical models predict that mimics with an intermediate similarity to several model species can be better protected than an accurate mimic of a single model species [14, 18], and thus increasing similarity to one model might come at the cost of lower accuracy to another. It is highly likely that predators will encounter more than one model species in their foraging, but the extent to which this influences inaccurate mimicry is not known [14, 15].

Finally, if selective pressures other than those imposed by predators influence the mimic's appearance, then inaccurate mimics could represent a trade-off between such opposing pressures. For example, increasing

similarity to the model may come with a physiological cost, such as reduced ability to regulate temperature. Hoverfly colour patterns are known to vary with temperature both seasonally and geographically [22], and this variation is thought to confer a survival advantage in response to differing thermoregulatory constraints [23]. In temperate climates, darker coloured insects are able to warm up more quickly [24, 25], and thus improve performance in areas such as flight activity [26]. It is highly plausible that such a mechanism underlies colour variation in hoverflies. However, to our knowledge, the effect of this variation on mimetic accuracy has never been assessed. We would expect to see a conflict in temperate regions between the bright colours required for mimicry and dark colours that allow effective temperature regulation.

Among the wealth of theories which seek to explain inaccurate mimicry, most have been studied through mathematical modelling or abstract experiments [2, 13]. Only recently has attention turned to a broader perspective of testing the various hypotheses against each other in real systems, which is the only way in which the relative merits of the different hypotheses can be accurately assessed. Penney et al. [21] carried out a comparative study of 38 hoverfly species, along with 10 putative models, using both morphological data and human judgment to measure degree of similarity. They found evidence that inaccurate mimics are not just artefacts of human perception, and suggested that no species are intermediate between several models. However, they found a positive relationship between size and mimetic accuracy, which they interpret as evidence for the relaxed selection theory, suggesting that larger hoverflies are more valuable prey and therefore under stronger selective pressure.

Another comparative study by Holloway et al. [19] investigated the levels of phenotypic variation in a number of hoverfly and wasp species. They used rankings of mimetic accuracy as calculated from behavioural responses of pigeons recorded in Dittrich et al. [6], and were consequently limited to the few species used in the pigeon study. Holloway et al. [19] found high levels of variation in many species, giving no indication that a lack of genetic variation was limiting the evolution of accuracy. They did not find a clear trend between mimetic accuracy and phenotypic variation, although particularly high variation in the model species and one accurate mimic, *Temnostoma vespiforme*, led them to conclude that relaxed selection may be acting in those cases.

The few empirical studies which have attempted to test predictions about variation in mimetic accuracy have been constrained by the difficulties of generating effective measures of similarity between mimics and their models. It is possible to use predator behaviour to rank similarity [e.g. 6], but this approach becomes prohibitively expensive if applied to large numbers of specimens, and so in large-scale studies, a mathematical similarity measure is essential. For example, Holloway et al. [19] characterized mimic phenotype simply using the proportion of yellow versus black on two tergites of the abdomen. The descriptors that Penney et al. [21] used to create a multivariate measure of mimetic accuracy included morphometric data (e.g. antenna length, thorax width, wing length) as well as some summary variables relating to the abdominal pattern (e.g. mean red-green-blue values, number of stripes), but very little about the pattern itself.

Recently, we have developed a new objective measure of mimetic accuracy by comparing entire abdominal patterns using the distance transform method [27]. This method is not intended as a faithful representation of a potential predator's cognitive processes, which in any case are not currently known, but as an objective means of capturing detailed information about pattern variation, beyond simple summary measures such as colour proportions. Nonetheless, our method provides a measure of mimetic accuracy much closer to human and avian estimates than previous empirical measures, even without the inclusion of any morphometric data [27]. In the current study, we use this new methodology to characterize the mimetic patterns of hoverflies in detail, and to test some of the predictions which have emerged from theoretical work. We plot a large number of model and mimic individuals in "similarity space", giving a picture not only of how species compare with one another in appearance, but also of the variation within species. We then test four predictions associated with three theoretical explanations for the existence of inaccurate mimicry:

1. Relaxed selection
    a. Lack of genetic variation: Less accurate mimics are under strong selection but lack the genetic variation to evolve increased accuracy; more accurate mimic species experience relaxed selection and thus have higher levels of phenotypic variation.
    b. Incentive to attack: Less accurate mimic species have higher levels of phenotypic variation since they provide a lower incentive to attack and are under more relaxed selection.

2. Multiple models: Increasing accuracy to one model decreases accuracy to others; inaccurate mimics represent a compromise between two or more model phenotypes.
3. Thermoregulation: Less accurate mimics have more black in their pattern and hence will be better able to regulate their temperature; there is a trade-off between accurate mimicry and effective thermoregulation.

METHODS

Image processing and dissimilarity calculations were carried out in MATLAB [28]. Statistical analyses were carried out in R version 3.0.3 [29].

Specimens

Insects were collected using a hand net from wild communities in Nottinghamshire, UK (particularly the Attenborough Nature Reserve) and surrounding areas, during May to October in the years 2012-2014. See Table S1 for full details of sampling sites. Target insects were any hoverflies or stinging Hymenoptera bearing a two-colour pattern (usually black and yellow; see example images in Figure S1), but excluding bumblebees and their putative mimics, which are notably much hairier than other the other taxa encountered (making automated characterization of the abdominal pattern difficult), and which are very likely part of a different mimicry ring [15]. We follow other studies such as [21] in excluding male Hymenoptera from the analysis as, not having a sting, their status as models is debatable (they may still be unpalatable to predators due to other factors [5]). Males are also of much lower abundance than females for most of the year, and thus only five specimens were excluded from this study. A total of 954 individuals were identified to species level and sexed using relevant keys [16, 17, 30].

Specimens were euthanised by freezing, and their legs and wings pinned out to the sides when necessary to give a clear view of the abdomen. They were then placed inside a homemade “photo studio” – a white 30 x 18 x 10 cm open topped box. A 5mm scale bar was placed near to the insect. Specimens were photographed from above with a Canon 600D DSLR camera and Tamron 90mm macro lens under natural outdoor light

conditions, in the shade. This method resulted in images that were evenly lit and free from strong reflections or glare. While natural weather variation did lead to some changes in brightness from image to image, this did not affect the analysis since patterns were converted to binary form before comparison (see "image processing").

Image processing

Images were rotated, cropped, and rescaled to a standard alignment, and an algorithm was applied to remove noise and sharpen edges. An edge detection algorithm was used to find the outline of the abdomen. In some cases, a rough outline was drawn manually and passed to the algorithm as a starting point, to fix cases where the outline was difficult to detect against the background.

The abdomen was automatically segmented into two colour regions (typically black and yellow/orange). Some images (129 out of 954) did not produce clear segmentations, often due to fading of the colours after death (C. Taylor 2012, pers. obs.) and were discarded from further analyses. To quantify the colour proportions in the pattern, we calculated the proportion of pixels within the abdominal image that were classified as "black" (i.e. the darker of the two segments) after segmentation.

See SI Text and Figure S2 for more detail on the image processing.

Mimetic accuracy

We calculated dissimilarity values for all possible pairings of images within the dataset using the distance transform method [27]. Optimization of the method used translation and scaling in the vertical direction to account for any slight misalignment of the patterns. For some subsequent figures and analyses, it is more intuitive to work with measures of mimetic accuracy than with dissimilarity. To make the conversion, we used the formula $A = 1 - (D / D_{max})$, where A is mimetic accuracy, D is dissimilarity and D_{max} is the largest dissimilarity value between any two individuals in the overall dataset. This scales mimetic accuracy to run from a minimum of 0 (defined by this particular dataset) to a maximum of 1 (independent of the dataset – identical images). For each individual mimic, we calculated the mean similarity with respect to all individuals of a given model species, to give a measure of mimetic accuracy to that model.

We first tested for sexual dimorphism in the hoverfly species, since males and females may have different levels of mimetic accuracy, or might even resemble different models. For example, it has been suggested that female *Eristalis arbustorum* are bee mimics, while the males mimic wasps [31]. For each mimic species in our dataset for which we have data on at least three males and three females, we tested for dimorphism in both size and pattern. For size, we carried out a Wilcoxon two-sample test on thorax width data. For pattern, we used distance-based multivariate analysis [32, 33] carried out in the program DISTLM5. This allows the equivalent of ANOVA to be carried out directly on distance (dissimilarity) data rather than having to ordinate the data first. Species were considered dimorphic if $p < 0.05$ for either of the above tests, in which case the sexes were treated separately in all subsequent analyses. For species where $p > 0.05$ for both size and pattern, and those with fewer than three individuals in one or other sex, data from males and females were pooled in subsequent analyses. We refer to these groupings as "Species or Sex Units", or SSUs.

The mimetic accuracy for an SSU was calculated as the mean of the individual values of mimetic accuracy within that SSU, again for each model species separately. We then assigned each SSU a "best" model, being the potential model for which it has the highest mean accuracy value. Four species of Hymenoptera were treated as the candidate models of the sampled community (Figure S1), being the only potential models that were common in our samples ($N > 3$): *Vespula vulgaris* (common wasp), *Vespula germanica* (German wasp), *Vespa crabro* (hornet) and *Apis mellifera* (honeybee). We know from both theory [34] and experiments [35] that a model's importance in shaping predator behaviour increases with its abundance, and therefore we have excluded eight low-abundance ($N \leq 3$) model species from the main analysis. However, we did also repeat our analysis including these rarer model species (see SI Text).

1. Relaxed selection

To quantify variation within SSUs, we first ordinated the dissimilarity data by using Principal Coordinates Analysis (PCoA) [36]. We chose this method of ordination, as opposed to non-metric multidimensional scaling, as we considered it important to use a method in which the resulting inter-point distances would be linearly related to the original distance matrix. We did this in order to preserve the magnitude of the variation in the dataset, despite the fact that PCoA assumes that distances between individuals are metric

(that is, they obey the triangle inequality), which is not always the case when using distances generated by the distance transform method [27].

On the basis of a scree plot, we chose the first four dimensions of the PCoA as the best representation of the data. Using these four dimensions, we calculated the centroid for each SSU, and then the distance, *z,* of each individual to its corresponding centroid. The mean of a group's *z* values provides a measure of within-group variability [33].

When testing the relationship between mimetic accuracy and within-taxon variability in accuracy, using raw similarity values as a measure of mimetic accuracy is not appropriate. If a model and mimic species overlap in phenotypic space, we risk creating a circular argument. Mimics that are more variable will inevitably show lower accuracy, since a greater spread in phenotypic space will lead to larger distances (on average) to the model phenotype. For this test, therefore, we used a different measure of mimetic accuracy that is not affected by the phenotypic variability. After ordination using PCoA, we calculated centroid points for mimic and model species and defined (in)accuracy as the distance from a mimic's centroid to the closest model centroid.

To test for an influence of mimetic accuracy on within-taxon variability, we ran a generalized least squares model (GLS) [37] in the R package "ape" version 3.1-1 [38]. GLS is equivalent to a general linear model, but with the inclusion of a correlation matrix derived from the species' phylogeny to control for relatedness among species. We used mean *z* value for an SSU as the response and mean mimetic accuracy and mean thorax width (plus their interaction) as predictors. Thorax width was included in the model as a proxy for size [39], because Penney et al. [21] argued that larger hoverflies should offer a larger "incentive to attack" due to their greater nutritional value. The width of the thorax at the base of the wings was measured in ImageJ [40] using the unprocessed images, using a 5 mm bar in each image to set the scale. Note that in the early stages of the project, photographs did not include a scale bar, and therefore in some cases (e.g. see Table S2) samples for size measurements are smaller than for other measures such as pattern.

We tested the model under two different evolutionary scenarios: Brownian motion (BM) evolution, and Ornstein-Uhlenbeck (OU) evolution (similar to BM, but traits are constrained towards an "optimum" value).

These different scenarios were represented by two different correlation matrices passed to the GLS model, calculated from a composite phylogeny (Figure S3) based on information from Rotheray and Gilbert [41] and Ståhls et al. [42]. For both females and males, the OU evolutionary model was found to be a significantly better fit to the data (females: Likelihood Ratio (LR) = 11.71, p = 0.0006; males: LR = 6.10, p = 0.014; both df = 1) and was used for subsequent analysis. We then used backwards stepwise model simplification with likelihood ratio tests to find the minimum adequate model. In order to allow for sexual dimorphism, we conducted two separate analyses, one with data from only female individuals, and the other with only males.

2. Multiple models

To test for a potential trade-off in similarity to multiple models, we tested within SSUs for correlation (using Pearson's r) in mimetic accuracy towards the four main model species. A negative correlation would imply that, for a given SSU, increasing similarity to one model comes at the cost of decreased similarity to another. We tested all SSUs for which we had data on at least six individuals.

3. Thermoregulation

We tested for a trade-off between accuracy and the extent of black in the pattern ("proportion black") using a Markov Chain Monte Carlo generalised linear mixed model, implemented in the R package "MCMCglmm" [43]. Again, this method allowed us to control for phylogenetic relatedness among species. Accuracy of individual mimics to their closest model was the response variable, logit transformed for normality of residuals. Fixed effects were the proportion black, thorax width, sex and season, along with all two-way interactions. Thorax width was included as a proxy for size (see above), which can have a major impact on thermoregulation [44]. Season was included because selection on thermoregulation may vary according to the time of year. We categorised season as "early" (to 8th August) or "late" (9th August onwards) splitting at the date of the median sample, which also fell roughly halfway between the first and last sampling days. We also conducted a more complex analysis in which time of year was treated as a continuous variable, including a quadratic term, which gave very similar results. Species was included as a random effect, and we calculated a covariance structure for the random effect based on the phylogenetic tree (Figure S3; also see

261 “relaxed selection” above). We used backwards stepwise model simplification based on p values to find the
262 minimum adequate model. Note that in Figure 2, proportion black and thorax width are binned for ease of
263 interpretation, but they were treated as continuous in the analysis.

264

265 RESULTS

266 We examined pattern similarity among 697 hoverfly (54 species) and 128 hymenopteran individuals (12
267 species). We found evidence for size dimorphism in seven of the mimic species in our dataset, and for
268 pattern dimorphism in a further eleven (Table S2), giving a total of 72 SSUs. Compared against the four most
269 abundant species of Hymenoptera from our samples, 51 SSUs were classed as mimics of *Vespula vulgaris*, 11
270 of *Apis mellifera*, seven of *Vespa crabro*, and three of *Vespula germanica*. The level of mimetic accuracy to
271 the assigned model varied from 0.55 to 0.87 (Table S3, Figure S4).

272 **1. Relaxed selection**

273 If inaccurate mimics have insufficient genetic variation to reach a level of protection at which selection
274 becomes relaxed, we predict a positive correlation between pattern variability within species and similarity
275 to the model. Alternatively, if less accurate mimic species provide a low incentive for predators to attack, for
276 example because of a low calorific value, we predict a negative correlation. However, after controlling for
277 shared ancestry, phenotypic variability was not significantly associated with either mimetic accuracy or body
278 size (thorax width) in either males or females (Table 1 and Figure 1; see also Table S4).

279 **2. Multiple models**

280 If mimetic accuracy is limited by a trade-off among similarities to several models, we predict that similarity
281 to different model species should be negatively correlated. However, almost all SSUs show either a
282 significant positive correlation or no significant correlation among similarity values to the four main model
283 species (Table S5). There was only one negative correlation with $p < 0.05$: in males of *Syrphus ribesii*,
284 accuracy to *Apis mellifera* was negatively correlated with accuracy to *Vespa crabro* ($r = -0.56$, $p = 0.009$, N =

21). Under the null hypothesis, if all tests were independent, we would expect 10 negative correlations through type I error on average.

3. Thermoregulation

If mimetic accuracy is limited by a trade-off with thermoregulation, we predict a negative correlation between similarity to the model and the proportion of the pattern that is black. Having controlled for shared ancestry, there is a significant negative interaction between proportion black and thorax width ($p = 0.040$; Table 2). When combined with the other estimated coefficients (Table 2) this indicates that those mimics with a greater proportion of black on their abdomen tend to be less accurate to their model, and that this trend is particularly strong in larger mimics (Figure 2). There is a significant effect of sex, with females in general being more accurate ($p < 0.001$). In addition, both proportion black ($p < 0.001$) and thorax width ($p < 0.001$) interact with sex, with females showing a weaker version of the trend described above. These trends observed in colour, size and sex are evident even having accounted for seasonal differences in mimetic accuracy (Table 2 and Figure 2; see also Tables S6-7 and Figure S5).

DISCUSSION

By comparing colour patterns using the distance transform method [27] we have been able to quantify in detail the mimetic relationships in a community of insects, including variation both within and among species. The lack of a trend between accuracy and phenotypic variation suggests that inaccurate mimics are not accounted for by the fact that they have not been able to evolve to the point of maximum protection (Prediction 1a) or by relaxed selection caused by a reduced incentive of predators to attack (Prediction 1b). Rather, the data suggest that inaccurate phenotypes represent the result of a trade-off between opposing selective pressures. A trade-off caused by selection for similarity to multiple models (Prediction 2) is not supported, but the results point towards a hitherto unexplored role for thermoregulation in limiting the adaptive value of increased accuracy (Prediction 3).

The absence of a trend in phenotypic variation with mimetic accuracy and the relatively high levels of phenotypic variation are broadly in line with the results from Holloway et al. [19]. Therefore, it seems unlikely that inaccurate mimics are limited by a lack of genetic variation. We cannot tell from these data how much of the variation is heritable; at least some will be attributable to measurement error, and some to phenotypic plasticity, as (for example) adult patterns are known to change with the temperature experienced by the puparium [45]. However, the few studies of the genetic component of pattern variation in hoverfly species found a high level of heritability in those cases [46, 47].

The relaxed selection hypothesis predicts that, above a certain level of similarity, any further improvements in mimetic accuracy are selectively neutral [18]. Penney et al. [21] found a correlation between size and morphometric similarity to the model, and argued that smaller prey items are less valuable, and so relaxed selection allows the persistence of inaccurate mimicry in smaller hoverflies. However, a predator's optimal diet depends not only on the calorific value of the prey but also on search and handling times [48], and it is not clear whether large hoverflies provide the best trade-off in that regard. Furthermore, although Penney et al. [21] found that larger hoverflies tend to be more similar to their models in terms of morphology, our results reveal a more complicated relationship between pattern similarity and size. There is no direct effect of size on accuracy (Table 2) although there is an interaction with the colour proportions of the abdomen (see below), and in the case of males, the smallest are indeed the least accurate (Figure 2). Most importantly though, our data show no association between phenotypic variation and either size or mimetic accuracy. While our results do not rule out the possibility that selection on mimicry in hoverflies may be relaxed, they do show that relaxed selection is not connected with a species' level of mimetic accuracy or its size, and thus cannot provide an explanation for the observed variation in mimetic accuracy.

We are left with the likely explanation that there is some kind of opposing selective pressure that is balanced against the advantage of increased mimetic accuracy. The multiple models hypothesis provides one possibility. In terms of shape, hoverflies are clearly distinct from Hymenoptera, with none occupying phenotypes intermediate to two or more model species [21]. In terms of pattern, the distinction is less clear. After ordination in 2D space, there are a large number of hoverfly individuals that, for example, occupy the space in between *Apis mellifera* and *Vespula* spp. (Figure S4), but distinguishing an adaptive explanation

from random placement is difficult. Crucially, for each species of mimic, there is either no correlation or a positive correlation among similarity values to each potential model species. This implies that, at least in terms of pattern, there is no multi-model trade-off: assuming the observed variation has an underlying genetic component, it would be possible for each mimic to improve its similarity to one or more models without compromising similarity to others. We cannot rule out multiple models having an influence on the phenotype of a mimic, but we can conclude that the multiple models hypothesis is not sufficient to explain the observed levels of inaccuracy.

In contrast, a trade-off between mimicry and thermoregulation is consistent with our data. Hoverflies maintain a temperature excess (a body temperature above that of the surrounding air) through a combination of basking and shivering [49]. Darker coloured insects absorb more solar radiation, and therefore can heat up more rapidly [24, 25], so we expect darker hoverflies to be at a fitness advantage in cooler conditions. More rapid temperature gain during basking will reduce the opportunity cost of thermoregulation as well as possibly reducing predation risk. In support of this, a number of hoverfly species have been found to show seasonal variation in their colour patterns, with darker morphs being more common outside the summer months [45], which is thought to have an adaptive function in relation to temperature regulation [23].

However, the results of our study show that the thermoregulatory benefits of darker patterns will also likely be associated with a reduction in mimetic accuracy. To be a perfect mimic of *Vespula vulgaris,* the most abundant model in our samples, would require the amount of black on the abdomen to be limited to 51%, but almost all hoverflies surveyed were above this value (Table S3). Aposematic signals are known to constrain temperature regulation, as observed in the moth *Parasemia plantagenis* [50]. Moths with more black on their body were able to warm up more quickly, but suffered increased predation due to a less effective warning signal. Thus it is highly plausible that hoverfly colour patterns are constrained by their thermoregulation function. By contrast, wasp abdominal patterns are likely to be less constrained, since they do not rely much on basking for thermoregulation; social wasps achieve a high temperature excess through endothermy before they even leave their nest [51].

Interestingly, we find that the constraint on the colour pattern seems to be stronger in larger individuals, as revealed by the significant interaction between the proportion black and size. Larger insects are able to maintain a higher temperature relative to the ambient, but have slower heating rates [52]. Thus any differences in rates of warming caused by colour are likely to have a greater effect on fitness in larger than in smaller insects, the latter being unable to depart far from ambient temperature and so rates of warming are less likely to be a relevant factor. Indeed, both theoretical predictions [44] and physical models [53] have shown that colour should have a greater effect on temperature in larger organisms.

We also show that female hoverflies tend to be significantly better mimics than males, suggesting that the evolutionary pressures experienced by the sexes on their appearance are different. A similar observation has been made in butterflies, with females of some species being closer in colour to their models than males [54, 55], and many others in which mimicry is entirely restricted to the females [56]. A number of reasons have been suggested to explain those differences, including increased vulnerability of females to predators [57], conflict with intra-sexual signalling in males [58], and facilitating species recognition during mating [55]. These possibilities merit further investigation in hoverflies.

An alternative explanation that is consistent with a trade-off between accuracy and colour ratio could be that darker patterns are more cryptic to predators. It is possible that, as well as affecting mimetic accuracy and thermoregulation, the abdominal colour ratio may also affect the conspicuousness of the pattern. This potential explanation has received little attention in the literature, but it seems likely that, due to their high levels of activity, hoverflies are conspicuous regardless of their exact colour pattern. Even non-mimetic hoverflies are not considered cryptic [12].

For models, our study focused on four common species of Hymenoptera which are often regarded as the targets of mimicry in European hoverfly communities [15], but we caught a number of other hymenopteran species in small numbers, which could potentially also serve as models. The lower abundance and/or visibility of these species during our collection suggests that predators too will encounter them at a low rate, and therefore their importance as models is likely lower than those species that are widespread and conspicuous [35]. Nonetheless, conclusions are similar when we incorporate these rarer model species into

388 the analysis (see SI Text). We also note that the four common model species from our study all increase in
389 abundance during late summer/early autumn, and that this change could potentially affect the dynamics of
390 the mimetic community. However, the relationship between colour and mimetic accuracy cannot be
391 explained by seasonal effects, since it was observed even after seasonal variation was taken into account.

392 The phenotypic correlations we have described are consistent with a trade-off between mimicry and
393 thermoregulation, but we acknowledge that, due to the comparative nature of this study, we have not been
394 able to test this trade-off directly. As we have discussed, the mechanisms that we suggest may be
395 responsible for the observed correlation are consistent with what is known about mechanisms of insect
396 thermoregulation. Further work is now needed to test the effects of colour variation on both predation and
397 temperature of hoverflies in an experimental setting. Comparison of mimetic communities from different
398 climates may also provide a fruitful means of examining the conflict between mimicry and thermoregulation
399 in more detail.

400 **Ethics**

401 Collection of insect specimens was approved by the Nottinghamshire Wildlife Trust.

402 **Data accessibility**

403 The original dataset on which our analyses were based is available in Table S8.

404 **Competing interests**

405 We have no competing interests.

406 **Authors' contributions**

407 CT collected and analysed data and wrote the first draft of the manuscript. CT, TR and FG conceived the
408 study and revised the manuscript. All authors gave final approval for publication.

409 **Acknowledgements**

410 We thank staff at the Attenborough Nature Reserve and Nottinghamshire Wildlife Trust for permission to
411 collect specimens, and Chris du Feu and Katie Threadgill for assistance with fieldwork. We thank several
412 anonymous referees for their insightful comments on previous versions of the manuscript.

413 **Funding**

414 This study received no external funding.

415

416 REFERENCES

417 [1] Darwin, F. 1887 *The Life and Letters of Charles Darwin, vol. 2*. London, UK, John Murray.
418 [2] Ruxton, G.D., Sherratt, T.N. & Speed, M.P. 2004 *Avoiding Attack: The Evolutionary Ecology of Crypsis,*
419 *Warning Signals, and Mimicry*. Oxford, Oxford University Press.
420 [3] Bates, H.W. 1862 XXXII. Contributions to an Insect Fauna of the Amazon Valley. Lepidoptera: Heliconidæ.
421 *Trans. Linn. Soc. Lond.* **23**, 495-566. (doi:10.1111/j.1096-3642.1860.tb00146.x).
422 [4] Oaten, A., Pearce, C.E.M. & Smyth, M.E.B. 1975 Batesian mimicry and signal detection theory. *Bull. Math.*
423 *Biol.* **37**, 367-387.
424 [5] Mostler, G. 1935 Beobachtungen zur frage der wespenmimikry [Observations on the question of wasp
425 mimicry]. *Zoomorphology* **29**, 381-454. (doi:10.1007/bf00403719).
426 [6] Dittrich, W., Gilbert, F., Green, P., Mcgregor, P. & Grewcock, D. 1993 Imperfect mimicry: a pigeon's
427 perspective. *Proc. R. Soc. Lond. B* **251**, 195-200.
428 [7] Mappes, J. & Alatalo, R.V. 1997 Batesian mimicry and signal accuracy. *Evolution* **51**, 2050-2053.
429 [8] Valkonen, J.K., Nokelainen, O. & Mappes, J. 2011 Antipredatory function of head shape for vipers and
430 their mimics. *PLoS ONE* **6**, e22272. (doi:10.1371/journal.pone.0022272).
431 [9] Hossie, T.J. & Sherratt, T.N. 2013 Defensive posture and eyespots deter avian predators from attacking
432 caterpillar models. *Anim. Behav.* **86**, 383-389. (doi:http://dx.doi.org/10.1016/j.anbehav.2013.05.029).
433 [10] Greene, H.W. & McDiarmid, R.W. 1981 Coral snake mimicry: does it occur? *Science* **213**, 1207-1212.

[11] Pekár, S. & Jarab, M. 2011 Assessment of color and behavioral resemblance to models by inaccurate myrmecomorphic spiders (Araneae). *Invertebr. Biol.* **130**, 83-90.

[12] Rotheray, G.F. & Gilbert, F. 2011 *The Natural History of Hoverflies*. Cardigan, UK, Forrest Text.

[13] Kikuchi, D.W. & Pfennig, D.W. 2013 Imperfect mimicry and the limits of natural selection. *Q. Rev. Biol.* **88**, 297-315. (doi:10.1086/673758).

[14] Edmunds, M. 2000 Why are there good and poor mimics? *Biol. J. Linn. Soc.* **70**, 459-466. (doi:10.1111/j.1095-8312.2000.tb01234.x).

[15] Gilbert, F. 2005 The evolution of imperfect mimicry. In *Insect Evolutionary Ecology* (eds. M. Fellowes, G. Holloway & J. Rolff), pp. 231-288. Wallingford, UK, CABI.

[16] Stubbs, A.E. & Falk, S.J. 2002 *British Hoverflies: An Illustrated Identification Guide*. Reading, UK, British Entomological and Natural History Society.

[17] Richards, O.W. 1980 *Scolioidea, Vespoidea and Sphecoidea; Hymenoptera, Aculeata*. London, UK, Royal Entomological Society of London.

[18] Sherratt, T.N. 2002 The evolution of imperfect mimicry. *Behav. Ecol.* **13**, 821-826.

[19] Holloway, G., Gilbert, F. & Brandt, A. 2002 The relationship between mimetic imperfection and phenotypic variation in insect colour patterns. *Proc. R. Soc. Lond. B* **269**, 411-416.

[20] Johnstone, R.A. 2002 The evolution of inaccurate mimics. *Nature* **418**, 524-526.

[21] Penney, H.D., Hassall, C., Skevington, J.H., Abbott, K.R. & Sherratt, T.N. 2012 A comparative analysis of the evolution of imperfect mimicry. *Nature* **483**, 461-464. (doi:http://www.nature.com/nature/journal/v483/n7390/abs/nature10961.html#supplementary-information).

[22] Holloway, G.J. 1993 Phenotypic variation in colour pattern and seasonal plasticity in Eristalis hoverflies (Diptera: Syrphidae). *Ecol. Entomol.* **18**, 209-217.

[23] Ottenheim, M.M., Wertheim, B., Holloway, G.J. & Brakefield, P.M. 1999 Survival of colour polymorphic *Eristalis arbustorum* hoverflies in semi field conditions. *Funct. Ecol.* **13**, 72-77.

[24] Kingsolver, J.G. 1987 Evolution and coadaptation of thermoregulatory behavior and wing pigmentation pattern in pierid butterflies. *Evolution* **41**, 472-490. (doi:10.2307/2409250).

461 [25] Willmer, P.G. & Unwin, D.M. 1981 Field analyses of insect heat budgets: Reflectance, size and heating
462 rates. *Oecologia* **50**, 250-255. (doi:10.1007/BF00348047).
463 [26] Ellers, J. & Boggs, C.L. 2004 Functional ecological implications of intraspecific differences in wing
464 melanization in *Colias* butterflies. *Biol. J. Linn. Soc.* **82**, 79-87. (doi:10.1111/j.1095-8312.2004.00319.x).
465 [27] Taylor, C.H., Gilbert, F. & Reader, T. 2013 Distance transform: a tool for the study of animal colour
466 patterns. *Methods Ecol. Evol.* **4**, 771-781. (doi:10.1111/2041-210x.12063).
467 [28] MATLAB. 2012 MATLAB. (Natick, Massachusetts, The Mathworks.
468 [29] R Core Team. 2014 R: A language and environment for statistical computing. (Vienna, Austria, R
469 Foundation for Statistical Computing.
470 [30] Perkins, R.C.L. 1919 The British species of *Andrena* and *Nomada*. *Transactions of the Entomological*
471 *Society of London 1919*, 218-319.
472 [31] Heal, J.R. 1981 Colour patterns of Syrphidae. III. Sexual dimorphism in *Eristalis arbustorum*. *Ecol.*
473 *Entomol.* **6**, 119-127. (doi:10.1111/j.1365-2311.1981.tb00600.x).
474 [32] Anderson, M.J. 2001 A new method for non-parametric multivariate analysis of variance. *Austral Ecol.*
475 **26**, 32-46. (doi:10.1111/j.1442-9993.2001.01070.pp.x).
476 [33] McArdle, B.H. & Anderson, M.J. 2001 Fitting multivariate models to community data: a comment on
477 distance-based redundancy analysis. *Ecology* **82**, 290-297. (doi:10.1890/0012-
478 9658(2001)082[0290:fmmtcd]2.0.co;2).
479 [34] Getty, T. 1985 Discriminability and the sigmoid functional response: how optimal foragers could stabilize
480 model-mimic complexes. *Am. Nat.* **125**, 239-256.
481 [35] Lindström, L., Alatalo, R.V. & Mappes, J. 1997 Imperfect Batesian mimicry—the effects of the frequency
482 and the distastefulness of the model. *Proc. R. Soc. Lond. B* **264**, 149-153.
483 [36] Legendre, P. & Legendre, L. 1998 *Numerical Ecology*. 2nd English ed. ed. Amsterdam, Elsevier.
484 [37] Grafen, A. 1989 The phylogenetic regression. *Philosophical Transactions of the Royal Society B:*
485 *Biological Sciences* **326**, 119-157. (doi:10.2307/2396904).
486 [38] Paradis, E., Claude, J. & Strimmer, K. 2004 APE: Analysis of Phylogenetics and Evolution in R language.
487 *Bioinformatics* **20**, 289-290. (doi:10.1093/bioinformatics/btg412).

488 [39] Gilbert, F. 1985 Morphometric patterns in hoverflies (Diptera, Syrphidae). *Proc. R. Soc. Lond. B* **224**, 79-
489 90. (doi:10.1098/rspb.1985.0022).
490 [40] Abràmoff, M.D., Magalhães, P.J. & Ram, S.J. 2004 Image processing with ImageJ. *Biophotonics*
491 *International* **11**, 36-42.
492 [41] Rotheray, G. & Gilbert, F. 1999 Phylogeny of Palaearctic Syrphidae (Diptera): evidence from larval
493 stages. *Zool. J. Linn. Soc.* **127**, 1-112. (doi:10.1111/j.1096-3642.1999.tb01305.x).
494 [42] Ståhls, G., Hippa, H., Rotheray, G., Muona, J. & Gilbert, F. 2003 Phylogeny of Syrphidae (Diptera) inferred
495 from combined analysis of molecular and morphological characters. *Syst. Entomol.* **28**, 433-450.
496 [43] Hadfield, J.D. 2010 MCMC methods for multi-response generalized linear mixed models: the
497 MCMCglmm R package. *Journal of Statistical Software* **33**, 1-22.
498 [44] Stevenson, R.D. 1985 The relative importance of behavioral and physiological adjustments controlling
499 body temperature in terrestrial ectotherms. *Am. Nat.* **126**, 362-386. (doi:10.2307/2461361).
500 [45] Holloway, G., Marriott, C. & Crocker, H.J. 1997 Phenotypic plasticity in hoverflies: the relationship
501 between colour pattern and season in *Episyrphus balteatus* and other Syrphidae. *Ecol. Entomol.* **22**, 425-432.
502 [46] Conn, D.L.T. 1972 The genetics of the bee-like patterns of *Merodon equestris*. *Heredity* **28**, 379-386.
503 [47] Heal, J.R. 1979 Colour patterns of Syrphidae I. Genetic variation in the dronefly *Eristalis tenax*. *Heredity*
504 **42**, 223-236.
505 [48] Pyke, G.H., Pulliam, H.R. & Charnov, E. 1977 Optimal foraging: a selective review of theory and tests. *Q.*
506 *Rev. Biol.* **52**, 137-154.
507 [49] Morgan, K.R. & Heinrich, B. 1987 Temperature regulation in bee- and waspmimicking syrphid flies. *J.*
508 *Exp. Biol.* **133**, 59-71.
509 [50] Hegna, R.H., Nokelainen, O., Hegna, J.R. & Mappes, J. 2013 To quiver or to shiver: increased
510 melanization benefits thermoregulation, but reduces warning signal efficacy in the wood tiger moth. *Proc. R.*
511 *Soc. Lond. B* **280**, 20122812. (doi:10.1098/rspb.2012.2812).
512 [51] Heinrich, B. 1984 Strategies of thermoregulation and foraging in two vespid wasps, *Dolichovespula*
513 *maculata* and *Vespula vulgaris*. *Journal of Comparative Physiology B* **154**, 175-180.
514 (doi:10.1007/BF00684142).

515 [52] Digby, P.S.B. 1955 Factors affecting the temperature excess of insects in sunshine. *J. Exp. Biol.* **32**, 279-
516 298.
517 [53] Shine, R. & Kearney, M. 2001 Field studies of reptile thermoregulation: how well do physical models
518 predict operative temperatures? *Funct. Ecol.* **15**, 282-288. (doi:10.1046/j.1365-2435.2001.00510.x).
519 [54] Su, S., Lim, M. & Kunte, K. 2015 Prey from the eyes of predators: Color discriminability of aposematic
520 and mimetic butterflies from an avian visual perspective. *Evolution* **69**, 2985-2994. (doi:10.1111/evo.12800).
521 [55] Llaurens, V., Joron, M. & Théry, M. 2014 Cryptic differences in colour among Müllerian mimics: how can
522 the visual capacities of predators and prey shape the evolution of wing colours? *J. Evol. Biol.* **27**, 531-540.
523 (doi:10.1111/jeb.12317).
524 [56] Kunte, K. 2009 Female-limited mimetic polymorphism: a review of theories and a critique of sexual
525 selection as balancing selection. *Anim. Behav.* **78**, 1029-1036.
526 (doi:http://dx.doi.org/10.1016/j.anbehav.2009.08.013).
527 [57] Ohsaki, N. 1995 Preferential predation of female butterflies and the evolution of Batesian mimicry.
528 *Nature* **378**, 173-175.
529 [58] Lederhouse, R.C. & Scriber, J.M. 1996 Intrasexual selection constrains the evolution of the dorsal color
530 pattern of male Black Swallowtail butterflies, Papilio polyxenes. *Evolution* **50**, 717-722.
531 (doi:10.2307/2410844).
532

533 FIGURE LEGENDS

534 Figure 1. The relationship between pattern variability (mean z value) of an SSU and its mimetic accuracy.

535

536 Figure 2. The effect of colour ratio on mimetic accuracy. Hoverfly individuals have been binned into three
537 size categories in equal proportions: small (thorax up to 2.5mm wide; solid line), medium (2.6 to 3.8mm;
538 dashed line) and large (3.9mm or more; dotted line), and five colour categories (up to 52% black, 53-59%
539 black, 60-66% black, 67-74% black, and 75% or more black). Error bars show ± standard error. Note
540 truncation of the y axis.

TABLES

Table 1. GLS models of within-species variability.

sex	predictor	likelihood ratio	p
Female			
	accuracy:size	0.1	0.748
	accuracy	0.82	0.365
	size	1.09	0.296
Male			
	accuracy:size	0.63	0.427
	accuracy	0.87	0.350
	size	0.73	0.392

The contribution of each predictor to the model was assessed using a likelihood ratio test. All tests had Δdf = 1. Sample size was 32 for females and 34 for males.

Table 2. MCMCglmm model of mimetic accuracy

predictor	posterior mean	pMCMC
intercept	1.34	<0.001
proportion black	0.158	0.614
thorax width	0.052	0.434
sex (F)	0.426	<0.001
season (late)	-0.090	0.066
proportion black: thorax width	-0.204	0.040
proportion black: sex (F)	0.396	<0.001
thorax width: sex (F)	-0.188	<0.001
sex (F): season (late)	0.053	0.030
thorax width: season (late)	0.045	<0.001
proportion black: season (late)		0.104

Accuracy was logit transformed for normality. SSU was included as a random effect, with a variance structure that accounts for phylogenetic relatedness. Backwards model selection was used on the basis of the p values. Posterior means are quoted for coefficients of all predictors present in the minimum adequate model. All factors have df = 1. N = 638.

555

556

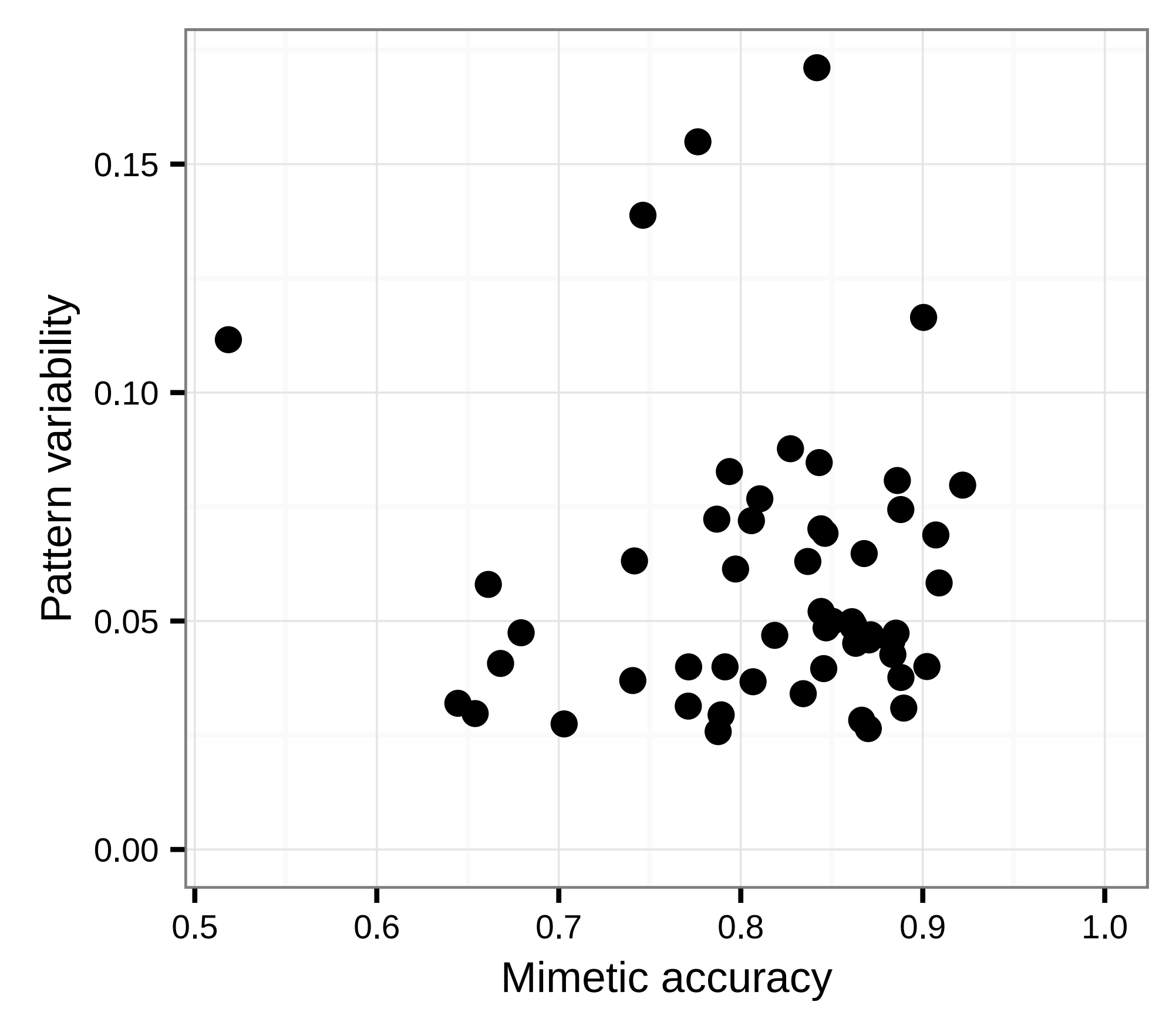
Pattern variability
0.15
0.10
0.05
0.00
0.5
0.6
0.7
0.8
0.9
1.0
Mimetic accuracy

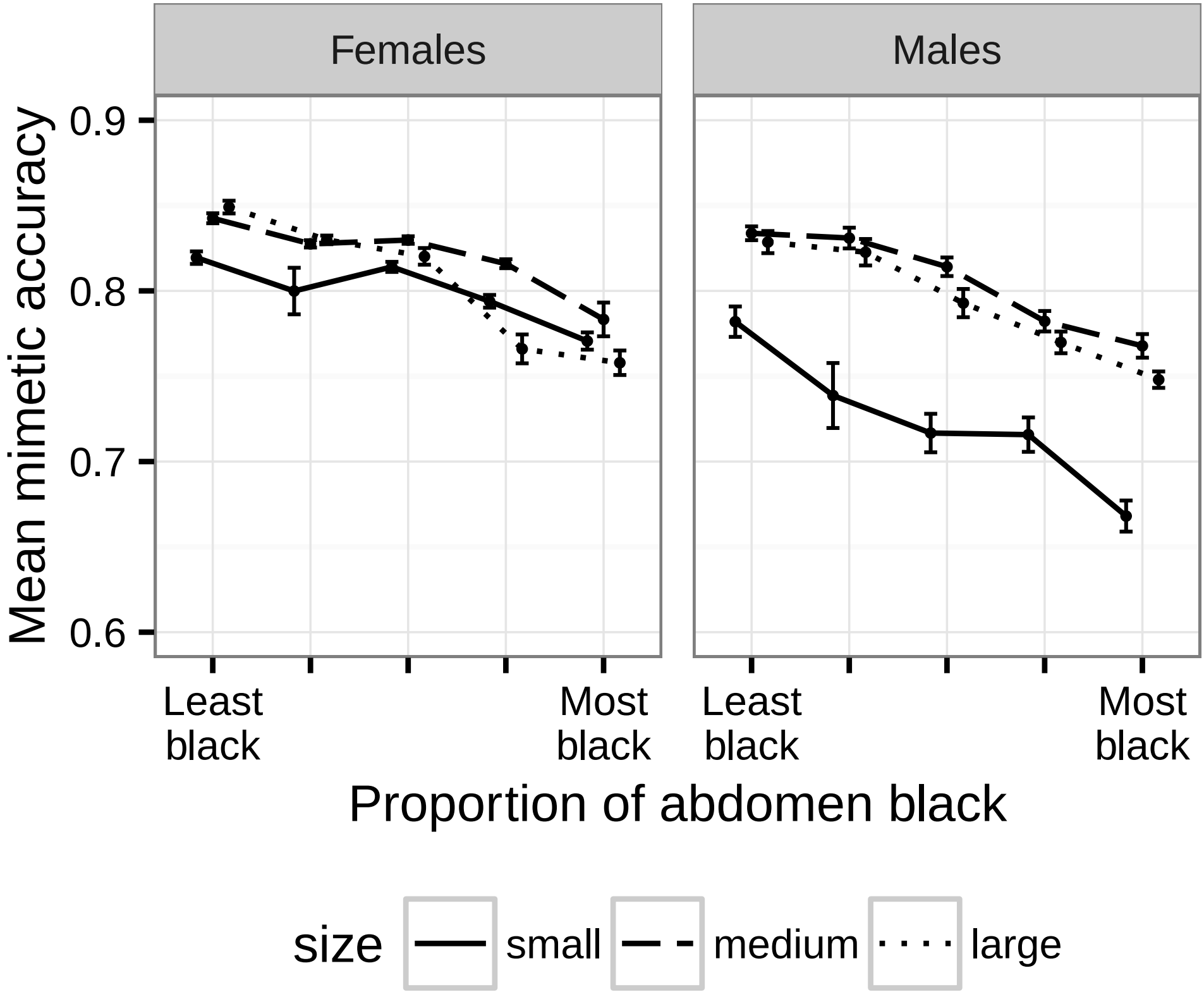
Females
Males
Mean mimetic accuracy
0.9
0.8
0.7
0.6
Least black
Most black
Least black
Most black
Proportion of abdomen black
size
small
medium
large

Why many Batesian mimics are inaccurate – Taylor, Reader and Gilbert 2016

Supporting information:

Supplementary methods – details of image processing (p. 1)

Supplementary results and discussion – rare model species (p. 3)

Figures S1-S5 (p. 4)

Tables S1-S7 (p. 9)

Table S8 is included as a separate file, and contains raw data for each individual insect

Supplementary methods – details of image processing

Image processing was carried out in MATLAB [1]. Three landmarks were selected by eye on each image (Figure S2A): 1, the tip of the abdomen, and 2 and 3, points at either side of the top of the abdomen. In hoverflies, 2 and 3 were located where the sides of abdominal tergite 2 met the scutellum, whilst in wasps, they were where the first tergite met the petiole. A further point, 4, was defined as the midpoint between 2 and 3, and the image rotated so that the line of symmetry running from 1 to 4 was vertical (with point 1 at the base). The image was also rescaled to fix the length of the abdomen at 100 pixels, and a smoothing algorithm was applied ["rotating mask"; 2] – see Figure S2B.

An edge detection algorithm then searched for an outline that joined 1 to 2 and 3, respectively (Figure S2C). In about half of all cases, this algorithm was effective in finding the outline of the abdomen (as checked by eye), but sometimes failed when “distracted” by other features in the image with a strong outline, such as legs lying close to the abdomen. In these latter cases, a “guide line” was drawn by eye, and then the algorithm was re-run, restricted to searching within 3 pixels of the guide (Figure S2D). This compromise between automated and user-driven processing allowed manual processing time and subjective input to be kept to a minimum whilst ensuring the effective separation of abdomen from background. The resulting outline, completed by a horizontal line across from the lower of points 2 and 3, defined the region of interest on which subsequent calculations were carried out.

The abdomen was segmented into two colour regions (typically black and yellow/orange; Figure S2E) using two alternative methods. For the first, the image was converted to greyscale by calculating the first principal component of the R, G and B values for all pixels. This resulted in a greyscale image in which the variation in brightness was maximised. This image was then segmented using a cut-off threshold calculated from Otsu’s method [3]. In the second method, for each pixel, the lowest of its three colour values (R, G or B) was subtracted from all three colour channels for that pixel, essentially giving its variation from grey, or saturation. The image was then converted to greyscale using principal components and segmented as in the first method.

Due to variation in colour among individual insects, as well as slight changes in lighting conditions among photographs, these two methods varied in their effectiveness at capturing the binary abdominal pattern. We therefore segmented each image using both methods and chose, by eye, the resulting segmentation that most closely represented the pattern as seen in the original image. Note that in many cases both methods produced a highly accurate segmentation and had only subtle differences. Some images (129 out of 968) did not produce good segmentations using either method and were discarded from further analyses.

To quantify the colour proportions in the pattern, we calculated the proportion of pixels within the abdominal image that were classified as “black” (i.e. the darker of the two segments) after segmentation.

[1] MATLAB. 2012 MATLAB. (Natick, Massachusetts, The Mathworks.
[2] Sonka, M., Hlavac, V. & Boyle, R. 2008 *Image Processing, Analysis, and Machine Vision*. Third ed, Thomson.
[3] Otsu, N. 1975 A threshold selection method from gray-level histograms. *Automatica* **11**, 285-296.

Supplementary results and discussion - rare model species

In addition to the four main model species analysed in the main text, we found eight further species of yellow-and-black Hymenoptera in our samples in small numbers: *Ancistrocerus trifasciatus* (N = 3), *Ectemnius cavifrons* (3), *Dolichovespula saxonica* (2), *Mellinus arvensis* (2), *Crossocerus binotatus* (1), *Ectemnius continuus* (1), *Nomada goodeniana* (1) and *Nomada marshamella* (1). We excluded these from the main analysis on the basis that they are unlikely to have much of an effect on predator learning in these communities due to their scarcity. However, it is possible that population sizes may have been different in the past, and therefore there is still the potential that they could have shaped the evolution of the mimics within the community.

Here we briefly present a parallel analysis to that presented in the main body of the paper (four models, or 4M), repeated using all twelve possible model species (12M).

1. Relaxed selection

As with the 4M analysis, none of the included predictors had a significant effect on pattern variability (Table S4).

2. Multiple models

Repeating this analysis with 12M rather than 4M greatly increases its complexity: rather than looking at six possible pairings of model species, we now have 66. There are 34 different SSUs for which we have data for six or more individuals, giving a total of 2244 tests of correlation. The scope for false positives is therefore high; even if none of the species have a true negative correlation, we would expect to detect a significant negative correlation in approximately 56 cases (2.5% of the total) if each test were independent.

In reality, we find only 30 examples of negative correlations, spread amongst 14 different mimic species. We can expect that at least the majority of these will be false positives. Even if a small scattering of genuine negative correlations do exist, which could indicate potential trade-offs in a few species, it appears that the community as a whole is not being shaped by these trade-offs.

3. Thermoregulation

This repeat analysis yields a similar set of predictors for mimetic accuracy, although the interaction between sex and season is no longer significant, while there is an interaction between proportion black and season (Table S6). Changes in the coefficients, once the interactions are taken into account, reflect a weaker effect of proportion black on accuracy. In this analysis, only the large males show a clear decrease in mimetic accuracy with increasing black in the pattern (Figure S5).

Supplementary Figures

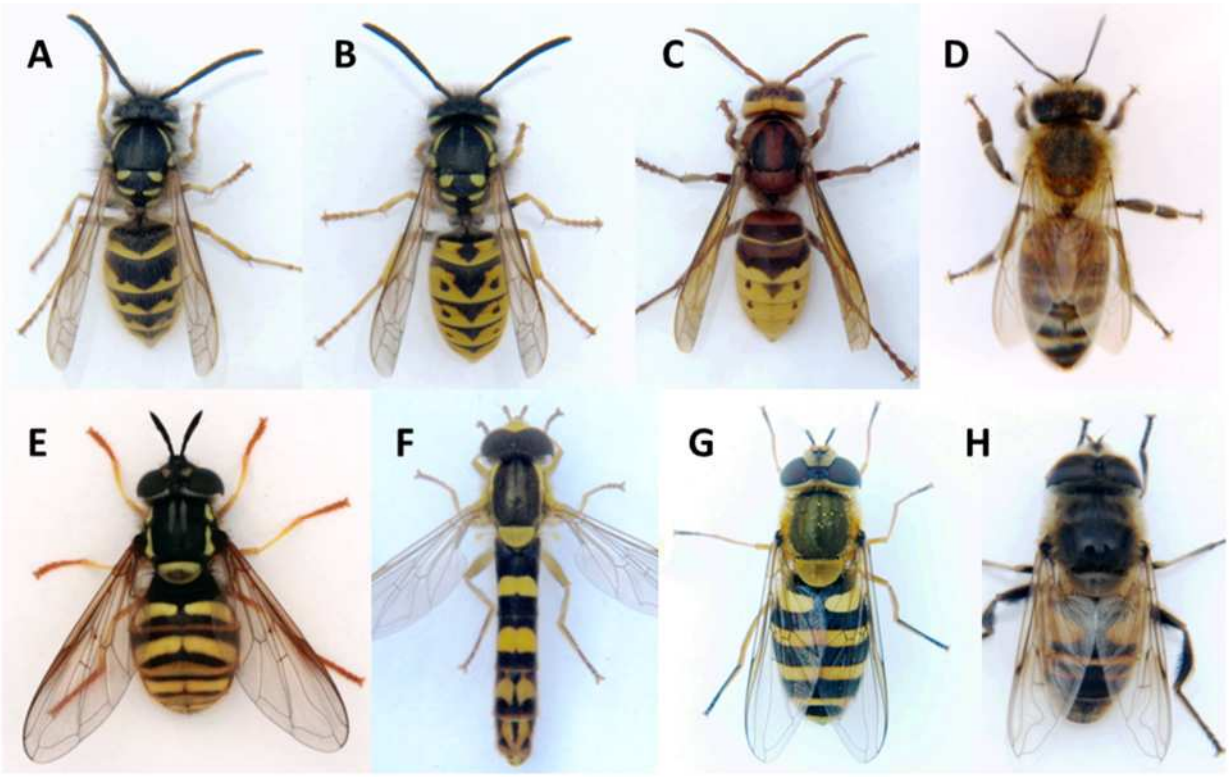

Figure S1. Photographs of live specimens of a selection of species that feature in this study. Hymenoptera: A *Vespula vulgaris*; B *Vespula germanica*; C *Vespa crabro*; D *Apis mellifera*. Syrphidae: E *Chrysotoxum arcuatum*; F *Sphaerophoria scripta*; G *Syrphus ribesii*; H *Eristalis tenax*.

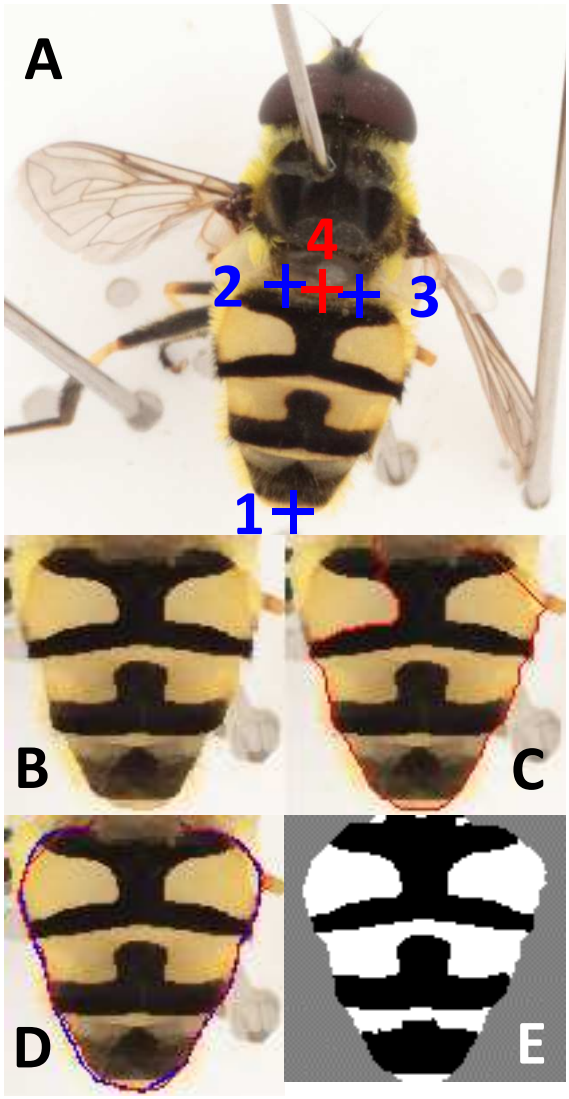

Figure S2. Image processing example (*Myathropa florea*). All steps were automated except those shown in blue. A: The user selects three control points on the image to identify the abdomen. A fourth point is calculated automatically as midway between 2 and 3. B: The image is scaled to a height of 100 pixels, cropped, rotated and smoothed. C: An edge detection algorithm is used to connect point 1 to 2 and 3. D: When necessary, the user draws a rough outline (blue) which is used to "guide" the edge detection algorithm to a more appropriate result (red). E: RGB pixel values are used to split the abdomen image into two "segments", one for yellow and one for black.

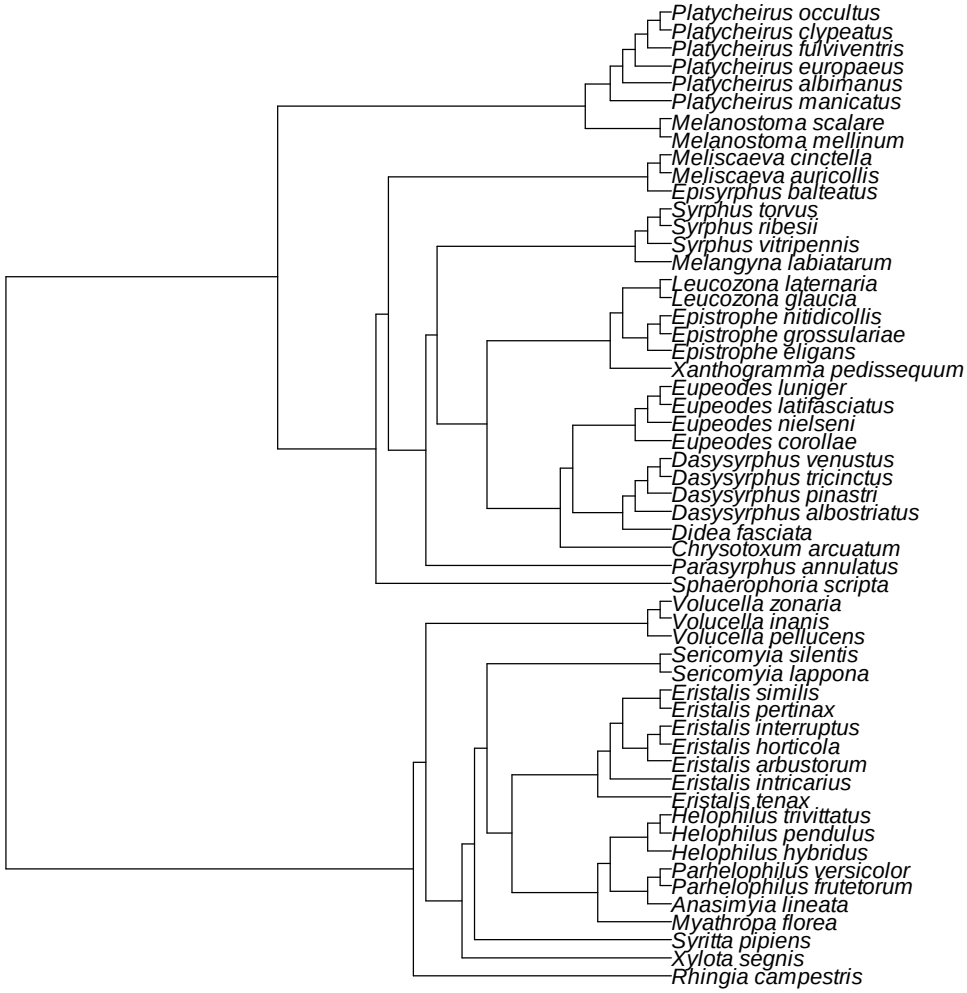

Figure S3. Phylogeny of the Syrphid species appearing in our samples. Used to control for relatedness among species in our analyses. This tree was assembled using data both morphological and molecular data (51 and 52). Branch lengths were assigned using Grafen's method (47).

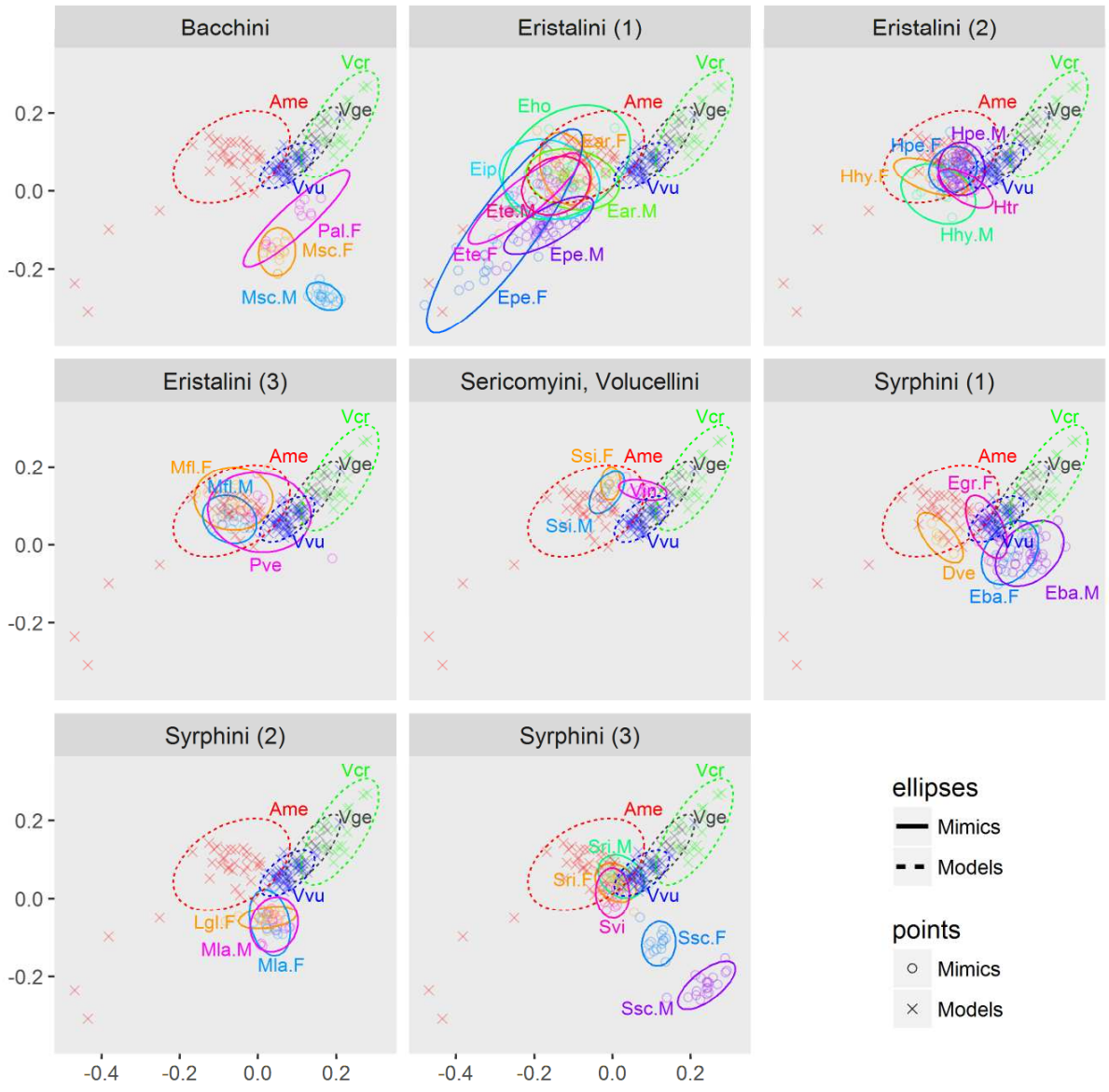

Figure S4. Models and mimics plotted in similarity space using the first two dimensions from CMDS. SSUs with N < 6 are not plotted. Ellipses show 95% confidence limits for each SSU, calculated from a modelled multivariate normal distribution based on the individual data points. SSUs are divided amongst panels according to their tribes and genera for clarity. See Table S2 for abbreviations.

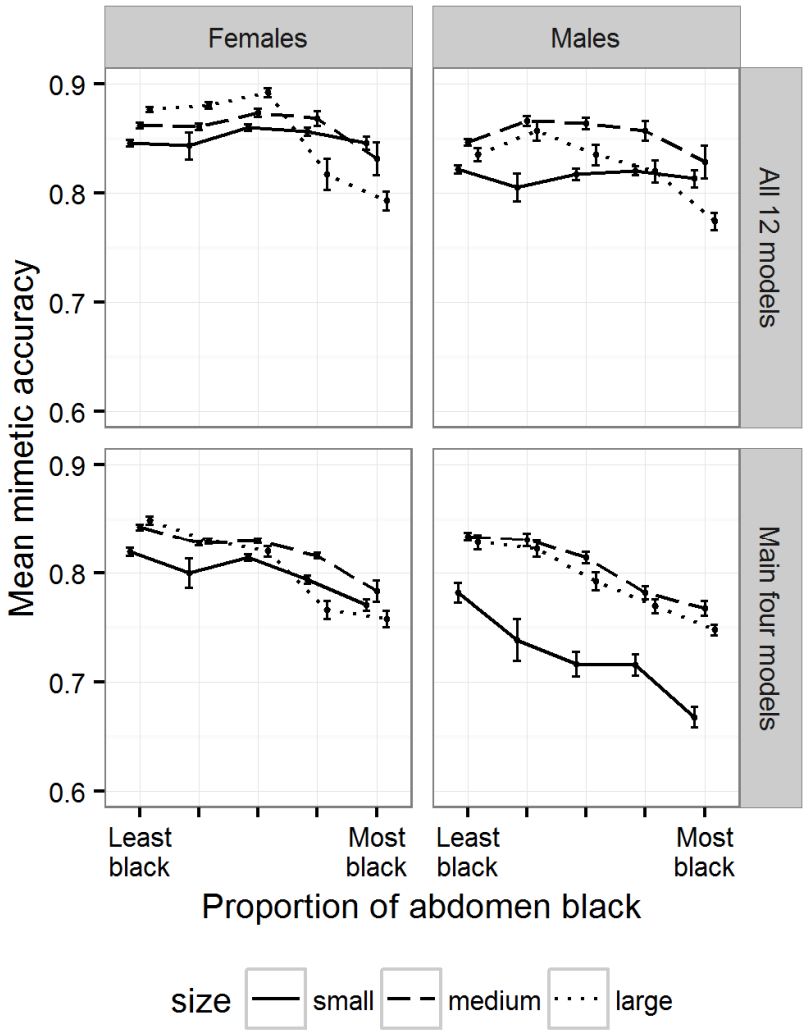

Figure S5. The effect of colour ratio on mimetic accuracy. Accuracy is calculated separately based on both all 12 models (top row) and the main four models (bottom row). Hoverfly individuals have been binned into three size categories in equal proportions: small (thorax up to 2.5mm wide; red), medium (2.6 to 3.8mm; green) and large (3.9mm or more; blue), and five colour categories (up to 52% black, 53-59% black, 60-66% black, 67-74% black, and 75% or more black). Error bars show ± standard error.

Supplementary Tables

Table S1. Brief descriptions of sampling sites used in this study. Note that totals are only for individuals that were included in the analysis – specimens for which images did not segment well are excluded.

Name	Latitude	Longitude	Description	Number of individuals
Attenborough Nature Reserve	52.91	-1.22	Wetland, former gravel pits	394
Cromford Canal	53.1	-1.53	Canal through deciduous woodland	131
Upper Moor	53.18	-1.54	Coniferous plantation	109
Grace Dieu Wood	52.76	-1.36	Deciduous woodland	84
Wollaton	52.96	-1.22	Allotment	30
University Lake	52.93	-1.2	Lakeside scrub	19
Piper Wood	52.79	-1.3	Deciduous woodland	17
Treswell Wood	53.31	-0.86	Deciduous woodland	12
Belton	52.78	-1.34	Rural garden	6
Shirland	53.12	-1.41	Rural garden	5
Dovedale Wood	53.07	-1.79	Deciduous woodland	5
Dovedale House	53.05	-1.8	Pasture	3
Harrow Road	52.95	-1.21	Suburban garden	3
Staunton Harold Reservoir	52.81	-1.44	Lakeside scrub	2
Calke Abbey	52.8	-1.46	Rural garden	2
Swineholes Wood	53.05	-1.93	Scrub/moorland	2
Monsal Dale	53.24	-1.71	Pasture	1

Table S2. Results for tests of sexual dimorphism, for those species with N ≥ 3 for both sexes. Size was tested using Wilcoxon two-sample test, and pattern was tested using distance-based ANOVA with a permutation test. Significant p values are highlighted in bold. * Numbers in brackets refer to N for size measurements.

Species	N* female	N* male	Size test: W	Size test: p	Pattern test: pseudo-F	Pattern test: p
Epistrophe grossulariae	16	3	38.5	0.112	10.45	**0.0009**
Episyrphus balteatus	17	37	106.5	**0.0001**	7.56	**0.0002**
Eristalis arbustorum	17 (16)	26	291.5	**0.030**	44.38	**0.0001**
Eristalis pertinax	26 (22)	47 (45)	332.5	**0.030**	37.95	**0.0001**
Eristalis tenax	9	15	94.5	0.109	7.65	**0.012**
Helophilus hybridus	7	7 (6)	28	0.351	28.61	**0.0001**
Helophilus pendulus	35 (32)	54 (52)	1091	**0.017**	25.51	**0.0001**
Helophilus trivittatus	3 (2)	4	-	-	2.24	0.147
Leucozona glaucia	18	4	38.5	0.862	4.25	**0.018**
Melangyna labiatarum	12 (6)	16 (2)	-	-	4.47	**0.016**
Melanostoma scalare	15	17 (15)	81	0.185	119.4	**0.0001**
Myathropa florea	18 (14)	14 (13)	69.5	0.306	5.64	**0.002**
Parhelophilus versicolor	3 (2)	10 (9)	-	-	2.6	0.080
Platycheirus albimanus	10	4	1	**0.008**	2.26	0.144
Platycheirus fulviventris	3	4	5	0.852	8.74	**0.003**
Sericomyia silentis	7	7	10.5	0.080	10.93	**0.0003**
Sphaerophoria scripta	14	19	86	0.086	51.44	**0.0001**
Syritta pipiens	4	4	16	**0.028**	18.04	**0.003**
Syrphus ribesii	24 (22)	21	149.5	**0.047**	7.3	**0.0002**
Syrphus vitripennis	12 (11)	6	16.5	0.102	2.7	0.056
Volucella pellucens	4	4	7.5	1.000	35.97	**0.008**

Table S3. Descriptive data for the model and mimic species sampled. Males and females are treated separately for sexually dimorphic mimic species (see Methods in main text). Models which were not included in the main analysis due to small sample size are listed in square brackets. These were also discounted when assigning the model for each mimic SSU. * N in brackets is the number of individuals with size recorded, where this differs from the total.

Species or Sex Unit	Abbrev.	Type	N*	Thorax width (mm)	Model	Accuracy	Proportion of the pattern that is black
Anasimiya lineata	Ali	Mimic	1	2.7	Vvu	0.833	0.64
Anicstrocerus trifasciatus	Atr	[Model]	3	2.2	-	-	0.70
Apis mellifera	Ame	Model	33 (25)	3.6	-	-	0.62
Chrysotoxum arcuatum	Car	Mimic	2	2.7	Vcr	0.848	0.46
Crossocerus binotatus	Cbi	[Model]	1	2.2	-	-	0.53
Dasysyrphus albostriatus	Dal	Mimic	4 (3)	2.5	Vvu	0.799	0.71
Dasysyrphus pinastri	Dpi	Mimic	1	2.6	Vvu	0.786	0.83
Dasysyrphus tricinctus	Dtr	Mimic	2	2.5	Vvu	0.809	0.84
Dasysyrphus venustus	Dve	Mimic	7 (6)	2.4	Ame	0.807	0.79
Didea fasciata	Dfa	Mimic	1	3.0	Vvu	0.830	0.62
Dolichovespula saxonica	Dsa	[Model]	2	3.0	-	-	0.64
Ectemnius cavifrons	Eca	[Model]	3	3.0	-	-	0.59
Ectemnius continuus	Ect	[Model]	1	2.8	-	-	0.73
Epistrophe eligans	Eel	Mimic	2 (0)	-	Ame	0.736	0.83
Epistrophe grossulariae F	Egr.F	Mimic	16	3.1	Vvu	0.820	0.54
Epistrophe grossulariae M	Egr.M	Mimic	3	2.9	Vvu	0.782	0.46
Epistrophe nitidicollis	Ent	Mimic	1 (0)	-	Vvu	0.848	0.58
Episyrphus balteatus F	Eba.F	Mimic	17	2.2	Vvu	0.828	0.48
Episyrphus balteatus M	Eba.M	Mimic	37	2.5	Vge	0.802	0.47
Eristalis arbustorum F	Ear.F	Mimic	17 (16)	3.5	Ame	0.798	0.77
Eristalis arbustorum M	Ear.M	Mimic	26	3.3	Vvu	0.789	0.64
Eristalis horticola	Eho	Mimic	9	3.6	Ame	0.791	0.68
Eristalis interruptus	Eip	Mimic	7	3.5	Ame	0.784	0.76
Eristalis intricarius	Eic	Mimic	5	4.4	Vvu	0.778	0.54
Eristalis pertinax F	Epe.F	Mimic	26 (22)	3.7	Ame	0.732	0.79
Eristalis pertinax M	Epe.M	Mimic	47 (45)	3.9	Ame	0.749	0.74
Eristalis tenax F	Ete.F	Mimic	9	4.5	Ame	0.780	0.78
Eristalis tenax M	Ete.M	Mimic	15	4.4	Ame	0.780	0.66
Eupeodes corollae	Eco	Mimic	4 (3)	2.2	Vvu	0.839	0.60
Eupeodes latifasciatus	Ela	Mimic	1	2.0	Vvu	0.833	0.55
Eupeodes luniger	Elu	Mimic	2	2.7	Vvu	0.813	0.69
Eupeodes nielseni	Enl	Mimic	3 (0)	-	Vvu	0.796	0.76
Helophilus hybridus F	Hhy.F	Mimic	7	3.8	Vvu	0.810	0.64
Helophilus hybridus M	Hhy.M	Mimic	7 (6)	3.6	Vvu	0.752	0.54
Helophilus pendulus F	Hpe.F	Mimic	35 (32)	3.4	Vvu	0.844	0.56
Helophilus pendulus M	Hpe.M	Mimic	54 (52)	3.2	Vvu	0.844	0.53
Helophilus trivittatus	Htr	Mimic	7 (6)	4.1	Vvu	0.833	0.54

Leucozona glaucia F	Lgl.F	Mimic	18	2.7	Vvu	0.802	0.67
Leucozona glaucia M	Lgl.M	Mimic	4	2.8	Vvu	0.785	0.70
Leucozona laternaria	Lla	Mimic	2	2.5	Vvu	0.762	0.75
Melangyna labiatarum F	Mla.F	Mimic	12 (6)	1.9	Vvu	0.830	0.73
Melangyna labiatarum M	Mla.M	Mimic	16 (2)	2.1	Vvu	0.800	0.73
Melanostoma mellinum	Mme	Mimic	4	1.7	Vvu	0.706	0.68
Melanostoma scalare F	Msc.F	Mimic	15	1.6	Vvu	0.755	0.76
Melanostoma scalare M	Msc.M	Mimic	17 (15)	1.7	Vvu	0.638	0.74
Meliscaeva auricollis	Mau	Mimic	1	2.0	Vvu	0.778	0.67
Meliscaeva cinctella	Mci	Mimic	3 (2)	1.9	Vvu	0.782	0.56
Mellinus arvensis	Mar	[Model]	2	2.2	-	-	0.60
Myathropa florea F	Mfl.F	Mimic	18 (14)	3.6	Vvu	0.817	0.59
Myathropa florea M	Mfl.M	Mimic	14 (13)	3.7	Vvu	0.833	0.60
Nomada goodeniana	Ngo	[Model]	1	3.1	-	-	0.57
Nomada marshamella	Nma	[Model]	1	3.2	-	-	0.73
Parasyrphus annulatus	Pan	Mimic	2	2.4	Vvu	0.755	0.56
Parhelophilus frutetorum	Pfr	Mimic	4 (2)	3.0	Vvu	0.860	0.56
Parhelophilus versicolor	Pve	Mimic	13 (11)	3.1	Vvu	0.866	0.56
Platycheirus albimanus F	Pal.F	Mimic	10	1.7	Vvu	0.797	0.63
Platycheirus albimanus M	Pal.M	Mimic	4	2.0	Vvu	0.735	0.70
Platycheirus clypeatus	Pcl	Mimic	4 (3)	1.7	Vvu	0.766	0.68
Platycheirus europaeus	Peu	Mimic	1	1.7	Vvu	0.747	0.79
Platycheirus fulviventris F	Pfu.F	Mimic	3	1.7	Vvu	0.778	0.46
Platycheirus fulviventris M	Pfu.M	Mimic	4	1.7	Vge	0.703	0.46
Platycheirus manicatus	Pma	Mimic	2	1.9	Vvu	0.774	0.67
Platycheirus occultus	Poc	Mimic	1	1.5	Vvu	0.756	0.74
Rhingia campestris	Rca	Mimic	3	2.5	Vcr	0.803	0.33
Sericomyia lappona	Sla	Mimic	3	3.7	Vcr	0.791	0.82
Sericomyia silentis F	Ssi.F	Mimic	7	4.3	Vcr	0.807	0.69
Sericomyia silentis M	Ssi.M	Mimic	7	4.6	Vcr	0.813	0.69
Sphaerophoria scripta F	Ssc.F	Mimic	14	1.6	Vvu	0.777	0.68
Sphaerophoria scripta M	Ssc.M	Mimic	19	1.7	Vvu	0.645	0.61
Syritta pipiens F	Spi.F	Mimic	4	2.1	Vvu	0.757	0.81
Syritta pipiens M	Spi.M	Mimic	4	1.7	Vvu	0.638	0.80
Syrphus ribesii F	Sri.F	Mimic	24 (22)	2.8	Vvu	0.830	0.62
Syrphus ribesii M	Sri.M	Mimic	21	2.9	Vvu	0.826	0.59
Syrphus torvus	Sto	Mimic	4	2.9	Vvu	0.828	0.62
Syrphus vitripennis	Svi	Mimic	18 (17)	2.4	Vvu	0.818	0.64
Vespa crabro	Vcr	Model	18 (17)	5.6	-	-	0.48
Vespula germanica	Vge	Model	14 (11)	3.4	-	-	0.40
Vespula vulgaris	Vvu	Model	47 (41)	3.0	-	-	0.51
Volucella inanis	Vin	Mimic	7	4.8	Vge	0.811	0.35
Volucella pellucens F	Vpe.F	Mimic	4	4.9	Ame	0.667	0.68
Volucella pellucens M	Vpe.M	Mimic	4	4.9	Ame	0.668	0.70
Volucella zonaria	Vzo	Mimic	2	6.1	Vcr	0.820	0.59
Xanthogramma pedissequum	Xpe	Mimic	1	2.5	Vvu	0.815	0.76

Xylota segnis	Xse	Mimic	4	2.6	Vcr	0.551	0.56

Table S4. Results of GLS analysis of pattern variability, with predictors accuracy, size and their interaction. Results are displayed for analysis that included all twelve model species as well as those for just the main four models.

		Main four models only		All model species	
sex	predictor	Likelihood ratio	p	Likelihood ratio	p
Females (N = 32)					
	accuracy:size	0.1	0.748	2.64	0.104
	accuracy	0.82	0.365	0.87	0.35
	size	1.09	0.296	0.43	0.512
Males (N = 34)					
	accuracy:size	0.63	0.427	0.08	0.78
	accuracy	0.87	0.35	1.66	0.197
	size	0.73	0.392	0.42	0.517

Table S5. Correlation (Pearson's r) within each SSU (with N ≥ 6) among similarity values to each of the four main model species. Significant correlations at $p < 0.05$ are highlighted in bold. Note that all but one of the significant correlations are positive.

SSU	N	*V. vulgaris* - *V.germanica*	*V. vulgaris* - *V.crabro*	*V. germanica* - *V. crabro*	*V. vulgaris* - *A. mellifera*	*V. germanica* - *A. mellifera*	*V. crabro* - *A. mellifera*
Dasysyrphus venustus	7	**0.96**	0.75	**0.76**	0.14	0.33	-0.02
Eristalis arbustorum F	17	**0.98**	**0.93**	**0.96**	**0.62**	**0.67**	**0.65**
Eristalis arbustorum M	26	**0.99**	**0.93**	**0.94**	0.19	0.15	0.00
Episyrphus balteatus F	17	**0.94**	**0.84**	**0.76**	**0.69**	**0.64**	0.31
Episyrphus balteatus M	37	**0.89**	**0.62**	**0.59**	**0.68**	**0.48**	0.04
Epistrophe grossulariae F	16	**0.89**	**0.62**	**0.72**	0.10	0.10	0.10
Eristalis horticola	9	**0.98**	**0.95**	**0.96**	**0.68**	**0.68**	0.54
Eristalis interruptus	7	**0.99**	**0.96**	**0.97**	0.72	**0.77**	0.69
Eristalis pertinax F	26	**1.00**	**0.98**	**0.99**	**0.91**	**0.92**	**0.86**
Eristalis pertinax M	47	**1.00**	**0.95**	**0.97**	**0.90**	**0.90**	**0.83**
Eristalis tenax F	9	**0.99**	**0.98**	**0.99**	**0.76**	**0.80**	**0.77**
Eristalis tenax M	15	**0.99**	**0.85**	**0.89**	0.35	0.29	-0.11
Helophilus hybridus F	7	**0.98**	**0.95**	**0.93**	0.74	**0.80**	**0.77**
Helophilus hybridus M	7	**0.95**	**0.81**	**0.93**	0.39	0.17	0.07
Helophilus pendulus F	35	**0.92**	**0.79**	**0.76**	0.00	-0.11	-0.10
Helophilus pendulus M	54	**0.93**	**0.72**	**0.79**	0.14	0.02	-0.11
Helophilus trivittatus	7	**0.91**	**0.82**	**0.84**	-0.10	-0.39	-0.12
Leucozona glaucia F	18	**0.97**	**0.85**	**0.82**	-0.27	-0.35	-0.30
Myathropa florea F	18	**0.97**	**0.82**	**0.88**	**0.57**	**0.54**	0.15
Myathropa florea M	14	**0.97**	**0.81**	**0.81**	-0.02	0.14	-0.22
Melangyna labiatarum F	12	**0.97**	**0.90**	**0.90**	0.26	0.37	0.30
Melangyna labiatarum M	16	**0.99**	**0.92**	**0.92**	0.45	0.44	0.35
Melanostoma scalare F	15	**0.99**	**0.91**	**0.90**	**0.74**	**0.71**	**0.73**
Melanostoma scalare M	17	**0.98**	**0.90**	**0.91**	**0.93**	**0.88**	**0.73**
Platycheirus albimanus F	10	**0.99**	**0.91**	**0.89**	0.00	-0.11	-0.05
Parhelophilus versicolor	13	**0.87**	**0.70**	**0.79**	0.16	-0.14	-0.27
Syrphus ribesii F	24	**0.89**	**0.91**	**0.85**	-0.07	0.01	-0.26
Syrphus ribesii M	21	**0.82**	**0.75**	**0.44**	-0.25	0.05	**-0.56**
Sphaerophoria scripta F	14	**0.98**	**0.90**	**0.88**	**0.79**	**0.73**	**0.77**
Sphaerophoria scripta M	19	**0.76**	**0.72**	**0.89**	0.45	0.00	0.05
Sericomyia silentis F	7	**0.89**	0.62	0.37	0.73	0.59	0.17
Sericomyia silentis M	7	**0.97**	0.44	0.46	-0.08	-0.08	-0.60
Syrphus vitripennis	18	**0.95**	**0.76**	**0.75**	0.41	0.44	0.14
Volucella inanis	7	**1.00**	**0.86**	**0.85**	0.36	0.33	0.17

Table S6. MCMCglmm model of mimetic accuracy, which has been logit transformed. This model treats time of year as a continuous variable, as compared to Table 2 of the main article, in which season was treated as a two-level factor. For this purpose, "day" is a signed continuous variable calculated as the number of days before or after 8th August. We include a quadratic term for "day" to allow for a mid-season peak. SSU was included as a random effect, with a variance structure that accounts for phylogenetic relatedness. Backwards model selection was used on the basis of the pMCMC values. Posterior means are quoted for all predictors present in the minimum adequate model. All factors have df = 1. N = 638.

predictor	posterior mean	pMCMC
intercept	1.29	<0.001
proportion black	0.17	0.570
thorax width	0.083	0.206
sex (F)	0.46	<0.001
day	-0.0011	0.238
day^2		0.394
proportion black: thorax width	-0.22	0.020
proportion black: sex (F)	0.38	<0.001
thorax width: sex (F)	-0.19	<0.001
sex (F): day	0.0013	0.004
thorax width: day	0.0007	0.022
proportion black: day		0.114
sex (F): day^2		0.808
thorax width: day^2		0.752
proportion black: day^2		0.312

Table S7. MCMCglmm model of mimetic accuracy, which has been logit transformed. This model uses accuracy estimates based on all twelve model species, as compared to Table 2 of the main article, which uses data from the four most abundant models only. SSU was included as a random effect, with a variance structure that accounts for phylogenetic relatedness. Backwards model selection was used on the basis of the pMCMC values. Posterior means are quoted for all predictors present in the minimum adequate model. All factors have df = 1. N = 638.

predictor	posterior mean	pMCMC
intercept	1.25	0.006
proportion black	0.79	0.048
thorax width	0.14	0.098
sex (F)	0.60	<0.001
season (late)	-0.32	0.002
proportion black: thorax width	-0.29	0.032
proportion black: sex (F)	0.29	0.048
thorax width: sex (F)	-0.11	<0.001
sex (F): season (late)		0.550
thorax width: season (late)	0.047	0.012
proportion black: season (late)	0.33	0.024